Inorganic Chemistry
Article

Inorg. Chem. **2011**, *50*, 1429–1440 **1429**
DOI: 10.1021/ic102061s

Discrete Rh^{III}/Fe^{II} and $Rh^{III}/Fe^{II}/Co^{III}$ Cyanide-Bridged Mixed Valence Compounds

Paul V. Bernhardt,[†] Manuel Martínez,*[,‡] Carlos Rodríguez,[‡] and Marta Vazquez[‡]

[†]*School of Chemistry and Molecular Biosciences, University of Queensland, Brisbane 4072, Australia, and* [‡]*Departament de Química Inorgànica, Universitat de Barcelona, Martí i Franquès 1-11, E-08028 Barcelona, Spain*

Received October 12, 2010

The heterotrinuclear complexes *trans*- and *cis*-[{*cis*-*VI*-$L_{15}Rh^{III}(\mu\text{-NC})$}{*trans*-*III*-$L_{14S}Co^{III}(\mu\text{-NC})$}$Fe^{II}(CN)_4]^{2+}$ are unprecedented examples of mixed valence complexes based on ferrocyanide bearing three different metal centers. These complexes have been assembled in a stepwise manner from their {*trans*-*III*-$L_{14S}Co^{III}$}, {*cis*-*VI*-$L_{15}Rh^{III}$}, and $\{Fe^{II}(CN)_6\}$ building blocks. The preparative procedure follows that found for other known discrete assemblies of mixed valence dinuclear Cr^{III}/Fe^{II} and polynuclear Co^{III}/Fe^{II} complexes of the same family. A simple slow substitution process of $[Fe^{II}(CN)_6]^{4-}$ on inert *cis*-*VI*-$[Rh^{III}L_{15}(OH)]^{2+}$ leads to the preparation of the new dinuclear mixed valence complex [{*cis*-*VI*-$L_{15}Rh^{III}(\mu\text{-NC})$}$Fe^{II}(CN)_5]^-$ with a redox reactivity that parallels that found for dinuclear complexes from the same family. The combination of this dinuclear precursor with mononuclear *trans*-*III*-$[Co^{III}L_{14S}Cl]^{2+}$ enables a redox-assisted substitution on the transient $\{L_{14S}Co^{II}\}$ unit to form [{*cis*-*VI*-$L_{15}Rh^{III}(\mu\text{-NC})$}{*trans*-*III*-$L_{14S}Co^{III}(\mu\text{-NC})$}$Fe^{II}(CN)_4]^{2+}$. The structure of the final *cis*-[{*cis*-*VI*-$L_{15}Rh^{III}(\mu\text{-NC})$}{*trans*-*III*-$L_{14S}Co^{III}(\mu\text{-NC})$}$Fe^{II}(CN)_4]^{2+}$ complex has been established via X-ray diffraction and fully agrees with its solution spectroscopy and electrochemistry data. The new species [{*cis*-*VI*-$L_{15}Rh^{III}(\mu\text{-NC})$}{*trans*-*III*-$L_{14S}Co^{III}(\mu\text{-NC})$}$Fe^{II}(CN)_4]^{2+}$ and [{*cis*-*VI*-$L_{15}Rh^{III}(\mu\text{-NC})$}$Fe^{II}(CN)_5]^-$ show the expected electronic spectra and electrochemical features typical of Class II mixed valence complexes. Interestingly, in the trinuclear complex, these features appear to be a simple addition of those for the Rh^{III}/Fe^{II} and Co^{III}/Fe^{II} moieties, despite the vast differences existant in the electronic spectra and electrochemical properties of the two isolated units.

Introduction

The assembly of preformed coordination compounds for their use as precursors in the formation of nanostructures, supramolecules or of metal−organic frameworks underpins contemporary coordination chemistry.[1,2] The unusual properties derived from the assembly of these components represents one of the driving forces of research in this area.[3] Such compounds exhibit interesting properties related with the recognition of biologically relevant compounds,[4] magnetic properties,[5] optical sensitivity,[6,7] catalysis,[8] and coupled electronic properties. In general all these novel properties are derived from a variable degree of cooperativity between the metal centers that comprise the assembly. With this in mind, it is clear that a comprehensive, reproducible, and predictable way of assembling such large compounds from simpler building blocks is essential. Although mechanistic synthetic strategies of mononuclear coordination compounds have been thoroughly studied and understood for many years,[9−11] the assembly of polynuclear coordination compounds is not known in the same detail. The irreproducibility,[12] as well as the reliance on X-ray crystallographic characterization of materials obtained from partially characterized mixtures, of some (or many) preparation procedures represents a serious bottleneck.

One of the simplest classes of polynuclear coordination compounds are mixed valence complexes.[13−16] These are formed from the assembly of redox active mononuclear components where one metal is capable of accepting an

*To whom correspondence should be addressed. E-mail: manel.martinez@qi.ub.es.

(1) Shojaee, K.; Edrissi, M.; Izadi, H. *J. Nanopart. Res.* **2010**, *12*, 1439–1447.
(2) Tas, M.; Yagan, M.; Bati, H.; Bati, B.; Büyükgüngör, O. *Phosphorus, Sulfur Silicon Relat. Elem.* **2010**, *185*, 242–248.
(3) Vilà, N.; Zhong, Y. W.; Henderson, J. C.; Abruña, H. D. *Inorg. Chem.* **2009**, *49*, 796–804.
(4) Ji, H.; Yeh, S. R.; Rousseau, D. L. *J. Biol. Chem.* **2004**, *279*, 9392–9399.
(5) Shatruk, M.; Avendano, C.; Dunbar, K. R. *Prog. Inorg. Chem.* **2009**, *56*, 155–334.
(6) Biancardo, M.; Schwab, P. F. H.; Argazzi, R.; Bignozzi, C. A. *Inorg. Chem.* **2003**, *42*, 3966–3968.
(7) D'Souza, F.; Ito, O. *Chem. Commun.* **2010**, 4913–4928.
(8) Qi, W.; Wang, Y.; Wu, L. *Chem.—Eur. J.* **2010**, *16*, 1068–1078.
(9) Schlessinger, G. G. *Inorganic Laboratory Preparations*; Chemical Publishing Company Inc.: Gloucester, MA, 1962.
(10) Brauer, G. *Handbook of Preparative Inorganic Chemistry*; Academic Press: New York, 1965; p 1737.
(11) Basolo, F. *Coord. Chem. Rev.* **1990**, *100*, 47–66.
(12) Bernhardt, P. V.; Martínez, M.; Rodríguez, C. *Inorg. Chem.* **2009**, *48*, 4787–4797.

Published on Web 12/29/2010

Chart 1

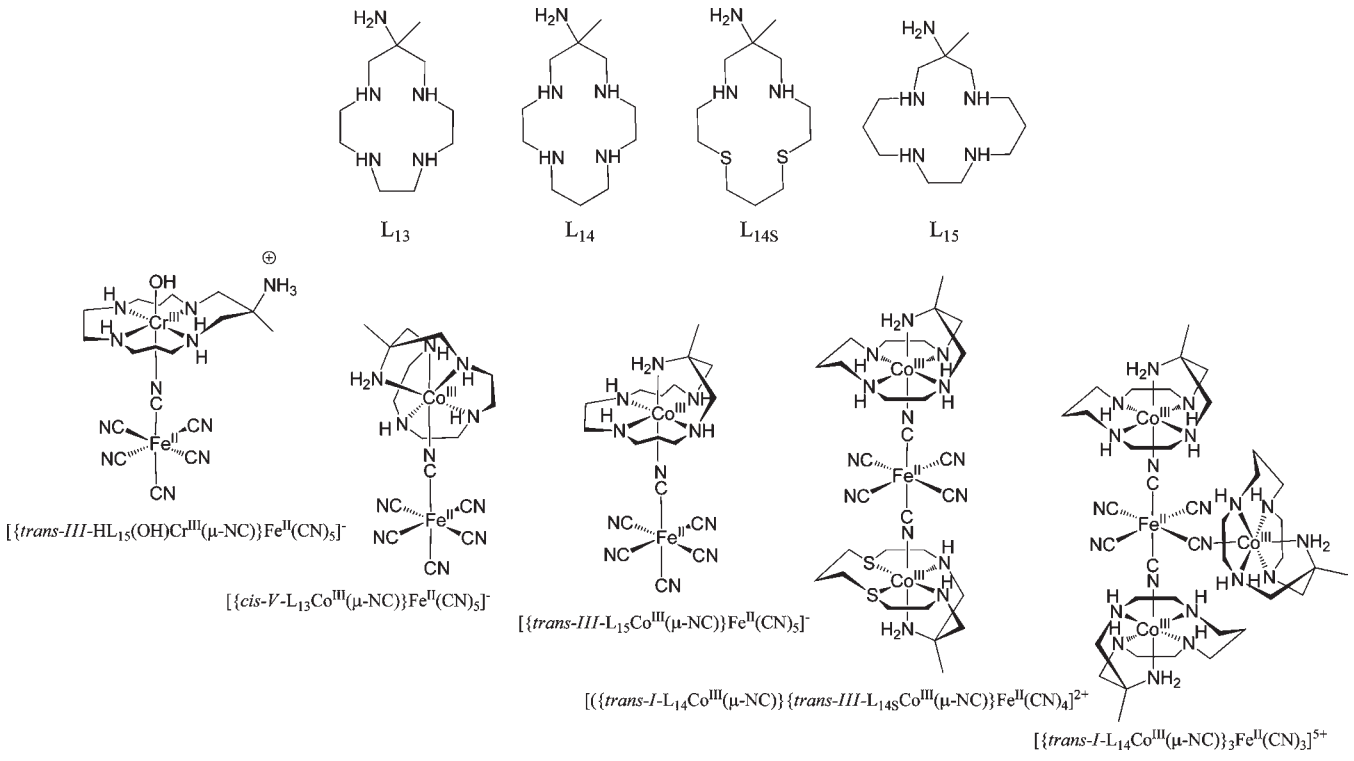

electron from the other through electronic excitation. As a result Class I, II, or III mixed valence complexes are formed (according to the degree of intermetallic coupling) with important differences in their electronic structure that are visualized in their magnetic and optical properties.

We have been involved in the preparation of Class II mixed valence heterodimetallic Co^{III}/Fe^{II} cyanide bridged complexes some of which are shown in Chart 1.[17] The Class II character of these complexes is associated with moderate electronic coupling between the metal centers that generates a metal-to-metal charge transfer (MMCT) electronic transition from the Fe^{II} to the Co^{III} center. The mechanistically driven preparation of these complexes has been studied in detail and careful tuning of redox potentials,[18−20] metal ion lability, solvent-assisted outer-sphere complexation, and building block isomerization processes have allowed accurate predictions of the outcome of such reactions.[12,21,22] Further, variations of both the cobalt and the iron coordination spheres has allowed a systematic tuning of the electronic properties of the series of the complexes.[23] Their redox reactivity has been investigated,[20,24,25] as well as their plausible involvement in dye-sensitized solar cells[26] or electrochromic materials.[27] Their encapsulation in silica gel matrixes has also been accomplished, and their use as easily removable catalysts for the formation of H_2O_2 has been also studied.[28] The use of these new dinuclear and inert building blocks for the assembly of mixed valence compounds with higher nuclearity has also been successfully pursued, and trinuclear ($Co^{III}{}_2/Fe^{II}$) and tetranuclear($Co^{III}{}_3/Fe^{II}$) complexes with different cobalt environments have been characterized.[12]

The use of analogous Cr^{III} mononuclear building blocks has also been investigated, and the same type of mixed valence Class II complexes can be prepared.[21] However, significant differences are observed with respect to the equivalent Co^{III}/Fe^{II} analogues. First, the mononuclear Cr^{III} building block reactivity is modified with respect to that of Co^{III}; the pendant arm of the L_{14} and L_{15} macrocycles becomes, de facto, a dangling protonated amino group in the mixed valence species (Chart 1). Second, electronic coupling between the $t_{2g}{}^6$ (Fe^{II}) and $t_{2g}{}^3$ (Cr^{III}) centers is much stronger (because of orbital symmetry),[13,16] as seen from the greater extinction coefficient of the associated MMCT band. Finally, the greater lability of the Cr^{II} center[29] complicates the formation of the final Cr^{III}/Fe^{II}

(13) Brunschwig, B. S.; Creutz, C.; Sutin, N. *Chem. Soc. Rev.* **2002**, *31*, 168–184.
(14) Creutz, C. *Prog. Inorg. Chem.* **1983**, *30*, 1–73.
(15) Lappin, A. G. *Redox Mechanisms in Inorganic Chemistry*; Ellis Horwood: Chichester, U.K., 1994.
(16) Robin, M. B.; Day, P. *Adv. Inorg. Chem. Radiochem.* **1967**, *10*, 247–422.
(17) Bernhardt, P. V.; Bozoglián, F.; Macpherson, B. P.; Martínez, M. *Coord. Chem. Rev.* **2005**, *249*, 1902–1916.
(18) Bernhardt, P. V.; Bozoglián, F.; Font-Bardía, M.; Martínez, M.; Meacham, A. P.; Sienra, B.; Solans, X. *Eur. J. Inorg. Chem.* **2007**, 5270–5276.
(19) Bernhardt, P. V.; Bozoglián, F.; Macpherson, B. P.; Martínez, M. *Dalton Trans.* **2004**, 2582–2587.
(20) Pérez-Tejada, P.; López-Pérez, G.; Prado-Gotor, R.; Sánchez, F.; González-Arjona, D.; López-López, M.; Bozoglián, F.; González, G.; Martínez, M. *Inorg. Chim. Acta* **2006**, *359*, 149–158.
(21) Basallote, M. G.; Bernhardt, P. V.; Calvet, T.; Castillo, C. E.; Font-Bardía, M.; Martínez, M.; Rodríguez, C. *Dalton Trans.* **2009**, 9567–9577.
(22) Martínez, M.; Pitarque, M. A.; van Eldik, R. *Inorg. Chim. Acta* **1997**, *256*, 51–59.
(23) Bernhardt, P. V.; Martínez, M.; Rodríguez, C. *Eur. J. Inorg. Chem.* **2010**, 5621–569.
(24) Bernhardt, P. V.; Bozoglián, F.; Macpherson, B. P.; Martínez, M.; González, G.; Sienra, B. *Eur. J. Inorg. Chem.* **2003**, 2512–2518.
(25) Bernhardt, P. V.; Bozoglián, F.; Macpherson, B. P.; Martínez, M.; Merbach, A. E.; González, G.; Sienra, B. *Inorg. Chem.* **2004**, *43*, 7187–7195.
(26) Bernhardt, P. V.; Boschloo, G. K.; Bozoglián, F.; Hagfeldt, A.; Martínez, M.; Sienra, B. *New J. Chem.* **2008**, *32*, 705–711.
(27) Bernhardt, P. V.; Kilah, N. L.; Meacham, A. P.; Meredith, P.; Vogel, R. *Dalton Trans.* **2005**, 2508–2515.
(28) Basallote, M. G.; Bozoglián, F.; Fernandez-Trujillo, M. J.; Martínez, M. *New J. Chem.* **2007**, *32*, 264–272.

Chart 2

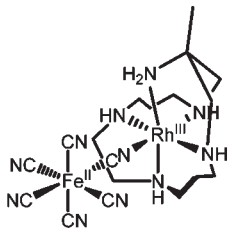

$[\{cis\text{-}VI\text{-}L_{15}Rh^{III}(\mu\text{-}NC)\}Fe^{II}(CN)_5]^-$

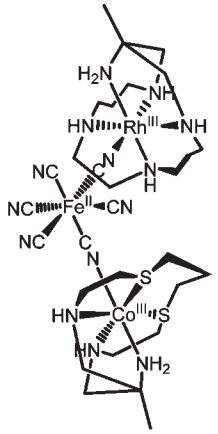

cis-$[(\{cis\text{-}VI\text{-}L_{15}Rh^{III}(\mu\text{-}NC)\}\{trans\text{-}III\text{-}L_{14S}Co^{III}(\mu\text{-}NC)\}Fe^{II}(CN)_4]^{2+}$

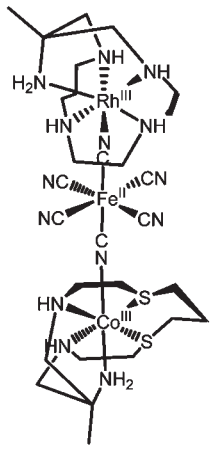

trans-$[(\{cis\text{-}VI\text{-}L_{15}Rh^{III}(\mu\text{-}NC)\}\{trans\text{-}III\text{-}L_{14S}Co^{III}(\mu\text{-}NC)\}Fe^{II}(CN)_4]^{2+}$

complex via the same mechanistically driven redox process,[22] and only direct substitution process on the Cr^{III} unit produces the desired final species.

In this paper we report the use of a more inert t_{2g}^6 Rh^{III} building block complex, *cis-VI*-$[RhClL_{15}]^{2+}$,[30] in the assembly of a new mixed valence compound, $[\{cis\text{-}VI\text{-}L_{15}Rh^{III}(\mu\text{-NC})\}Fe^{II}(CN)_5]^-$ (Chart 2). In this case, the combination of inertness and irreversibility of the Rh^{III} reduction process, makes a redox-assisted substitution process (via a Rh^{II}:Fe^{III} intermediate) unfeasible, and this presents synthetic challenges.[29,31] The alternative approach taken here is similar to that adopted for Cr^{III} analogues where redox reactions are avoided,[21] with the further advantage that the undesired photochemical processes occurring on these Cr^{III} compounds do not apply.[32,33] We also extend this approach to the assembly of heterotrinuclear (Rh^{III}:Fe^{II}:Co^{III}) complexes linked by cyanido ligands.

Experimental Section

Caution! *Although we have experienced no problems with the compounds in this work, perchlorate salts are potentially explosive and should only be handled in small quantities, never scraped from sintered glass frits, or heated while in the solid state.*

Preparation of Compounds. The complex *cis-VI*-$[RhClL_{15}](ClO_4)_2$ was prepared according to literature methods.[30] UV−vis and ^{13}C NMR spectroscopy established its isomeric configuration, and no other isomeric forms of the compound were evident during the ion-chromatography purification procedures.

Compound $Na[\{cis\text{-}VI\text{-}L_{15}Rh^{III}(\mu\text{-NC})\}Fe^{II}(CN)_5]$ was prepared using the same substitution procedure established for $Na[\{(HL_{15})(OH)Cr^{III}(\mu\text{-NC})\}Fe^{II}(CN)_5]$,[21] while taking into account the increased inertness of the Rh^{III} center. *cis-VI*-$[RhClL_{15}](ClO_4)_2$ (6×10^{-3} mol) was dissolved in water (500 cm^3), and the pH was adjusted to 12 with 2 M NaOH. After allowing the Cl^-/OH^- substitution reaction to conclude (ca. 30 min at 25 °C) a solution of 6×10^{-3} mol of $Na_4[Fe(CN)_6]$ in water (300 cm^3) was added, and the mixture kept at 70 °C for 18 h. After dilution of the reacted mixture to 8 dm^3 the solution was loaded onto a Sephadex DEAE-25 anion exchange chromatography column in perchlorate form. After repetitive washing of the column with water to remove cationic and neutral species, the product was eluted with 0.1 M $NaClO_4$. Concentration of the eluate on a rotary evaporator and then addition of acetone gave precipitation of a crude yellow solid. This was collected, dissolved in 250 cm^3 of water, and the chromatographic and precipitation procedures repeated. The solid obtained analyses as $C_{18}N_{11}H_{29}RhFeNa \cdot 8/5H_2O$: C 29.44 calc. (29.36 found) %; N 20.98 calc. (20.47 found) %; H 6.31 cal. (5.77 found) %. Yield 40%. Characterization was carried out also via UV−vis, IR, NMR, and electrochemistry. UV−vis, λ_{max} /nm (ε/M^{-1} cm^{-1}): 312 (1410), 352sh (1120). IR, $\bar{\nu}_{(CN)}/cm^{-1}$: 2045, 2078, 2118. NMR ^1H (400 MHz, D_2O, 298 K), δ/ppm: 1.38 (s, 3 H, CH_3); 1.80−3.60 (m, 20 H, CH_2); ^{13}C (100 MHz, D_2O, 298 K), δ/ppm: 21.4; 26.8; 30.9; 51.7; 52.5; 53.7; 54.8; 55.6; 57.2; 62.9; 63.8; 66.3; 176.8; 178.6 (×4); 184.1. Electrochemistry (mV versus NHE): +630 ($Fe^{III/II}$).

Compound $[\{cis\text{-}VI\text{-}L_{15}Rh^{III}(\mu\text{-NC})\}\{trans\text{-}III\text{-}L_{14S}Co^{III}(\mu\text{-NC})\}Fe^{II}(CN)_4](ClO_4)_2$ was prepared using the same procedure established for the known $[\{trans\text{-}II\text{-}L_{14}Co^{III}(\mu\text{-NC})\}\{trans\text{-}III\text{-}L_{14S}Co^{III}(\mu\text{-NC})\}Fe^{II}(CN)_4](ClO_4)_2$[12] using $[\{cis\text{-}VI\text{-}L_{15}Rh^{III}(\mu\text{-NC})\}Fe^{II}(CN)_5]^-$ and *trans-III*-$[CoCL_{14S}]^{2+}$ as starting materials. An aqueous solution 3×10^{-3} M in both complexes (100 cm^3) at a resulting pH of 4.5 was reacted at room temperature for 3 h, the mixture was diluted 5-fold and loaded on a Sephadex C-25 cation-exchange column. Under these conditions two cationic species eluted separately with 0.1 M $NaClO_4$. They were each concentrated to small volume (ca. 10 cm^3) at room temperature on a rotary evaporator, and addition of acetone (ca. 250 cm^3) yielded two solids in equal amounts.[32,33]

The solid from the first band (35% yield) was characterized as *trans*-$[\{cis\text{-}VI\text{-}L_{15}Rh^{III}(\mu\text{-NC})\}\{trans\text{-}III\text{-}L_{14S}Co^{III}(\mu\text{-NC})\}Fe^{II}(CN)_4]^{2+}$. ^{13}C NMR (D_2O): *cis-VI*-L_{15}: 21.4; 26.8; 30.9; 51.7; 52.5; 53.7;54.8; 55.6; 57.2; 62.9; 63.8; 66.3 ppm; *trans-III*-L_{14S}: 21.8; 28.1; 34.5; 44.0; 58.4; 68.1; 71.6 ppm; cyanides: 174.7(×4), 180.9, 191.5 ppm). The peaks indicate the presence of both *cis-VI*-L_{15} and *trans-III*-L_{14S} ligands,[19,30,36,36,37] as well

(29) Ducommun, Y.; Merbach, A. E. *Inorganic High Pressure Chemistry*; Elsevier: New York, 1986; Chapter 2, pp 69−114.
(30) Lawrance, G. A.; Martínez, M.; Skelton, A. W.; van Eldik, R.; White, A. H. *Aust. J. Chem.* **1992**, *45*, 351–359.
(31) Curtis, N. J.; Lawrance, G. A.; Sargeson, A. M. *Aust. J. Chem.* **1983**, *36*, 1327–1339.
(32) Stochel, G. *Polyhedron* **1994**, *13*, 155–157.
(33) Roundhill, D. M. *Photochemistry and Photophysics of Metal Complexes*; Plenum: New York, 1994.
(34) Bernhardt, P. V.; Martínez, M. *Inorg. Chem.* **1999**, *38*, 424–425.
(35) Bernhardt, P. V.; Bozoglián, F.; González, G.; Martínez, M.; Macpherson, B. P.; Sienra, B. *Inorg. Chem.* **2006**, *45*, 74–82.
(36) Aullón, G.; Bernhardt, P. V.; Bozoglián, F.; Font-Bardía, M.; Macpherson, B. P.; Martínez, M.; Rodríguez, C.; Solans, X. *Inorg. Chem.* **2006**, *45*, 8551–8562.
(37) Bernhardt, P. V.; Macpherson, B. P.; Martínez, M. *J. Chem. Soc., Dalton Trans.* **2002**, 1435–1441.

as three cyanido ligand carbon signals indicative of its *trans*-geometry. Anal. Calc. (found) for *trans*-[{*cis-VI*-$L_{15}Rh^{III}$(μ-NC)}{*trans-III*-$L_{14S}Co^{III}$(μ-NC)}$Fe^{II}(CN)_4](ClO_4)_2\cdot 5H_2O\cdot(CH_3)_2$-CO: C 30.62 (30.52) %, N 16.19 (16.39) %, H 5.80 (5.92) %, S 5.27 (4.98) %. Electrochemistry (mV versus NHE): +860 ($Fe^{III/II}$), −300 ($Co^{III/II}$). Electronic spectrum in water (λ_{max} / nm(ε /M^{-1} cm^{-1})): 284(17000), 352(1270), 462(595), 540(555). IR ($\bar{\nu}_{CN}$ /cm^{-1}): 2130, 2101, 2052.

The solid from the second band (20% yield) was characterized as *cis*-[{*cis-VI*-$L_{15}Rh^{III}$(μ-NC)}{*trans-III*- $L_{14S}Co^{III}$(μ-NC)}$Fe^{II}(CN)_4]^{2+}$. The ^{13}C NMR signals of the *cis-VI*-L_{15} and *trans-III*-L_{14S} ligands stated above were the only ones present in the saturated carbon region, but in the cyanide carbon region the spectrum shows five predominant signals at 173.4 (× 2), 175.2, 180.2, 185.2, and 188.7 ppm indicative of a *cis* arrangement of the two {M^{III}L} moieties. Anal. Calc. (found) for *cis*-[{*cis-VI*-$L_{15}Rh^{III}$(μ-NC)}{*trans-III*-$L_{14S}Co^{III}$(μ-NC)}Fe^{II}-$(CN)_4](ClO_4)_2\cdot 11H_2O$: C 27.26 (27.50) %, N 15.34 (15.27) %, H 5.70 (5.40) %, S 5.01 (4.75) %. Electrochemistry (mV versus NHE): +860 ($Fe^{III/II}$), −280 ($Co^{III/II}$). Electronic spectrum in water (λ_{max} /nm(ε /M^{-1} cm^{-1})): 284(17000), 354(1300), 462(540), 550(550). IR ($\bar{\nu}_{CN}$ /cm^{-1}): 2124, 2093, 2074, 2064, 2058, 2039. Slow evaporation of an aqueous solution of the solid produced crystals suitable for X-ray work.

Physical Methods. NMR spectra of vacuum-dried samples were recorded on a Varian Mercury-400 (^{1}H, 400 MHz or ^{13}C 100.6 MHz) instrument in D_2O/H_2O (8/2 to 2/8) and using NaTSP as external standard at the *Serveis Científico-Tècnics de la Universitat de Barcelona*. Elemental analyses were carried out by the *Serveis Científico-Tècnics de la Universitat de Barcelona*. UV−vis spectra were recorded on HP5483, Cary50 or J&M TIDAS instruments depending on the circumstances, as indicated. IR spectra were recorded on a Nicolet 520 FT-IR instrument as KBr disks. Electrochemistry experiments were carried out with PAR EG&G 263A or BioLogic SP-150 instruments using a glassy carbon working electrode, a Ag/AgCl (3 M KCl) reference electrode, and platinum wire counter electrode on 1×10^{-3} M solutions of the sample and using 1.0 M $NaClO_4$ as supporting electrolyte, unless otherwise stated. All potentials are given versus NHE, once corrected for the reference electrode used ($E°$ Ag/AgCl = +196 mV versus NHE).

Crystallography. Data were measured on an Oxford Diffraction Gemini CCD diffractometer using Cu−Kα radiation (1.5418 Å). Data reduction was performed with the CrysAlisPro programs (Oxford Diffraction, v. 171.33.44). The structure was solved by direct methods with SHELXS and refined by full-matrix least-squares analysis with SHELXL-97[38] within the WinGX graphical interface.[39] All non-H atoms were refined with anisotropic thermal parameters except for disordered perchlorate and water O-atoms. Alkyl and amino H-atoms were included at estimated positions using a riding model. Water H-atoms were not located. The molecular structure diagram was produced with ORTEP3.[40] Crystal and refinement data are summarized in Supporting Information, Table S1, and selected bond lengths appear in the caption of Figure 7.

Kinetics. All reactions were followed by UV−vis spectroscopy in the full 800−300 nm range. Observed rate constants were derived from the absorbance versus time traces at wavelengths where a maximum increase and/or decrease of absorbance was observed.[41] No dependence of the observed rate constant values on the selected wavelengths was detected, as expected for reactions where a good retention of isosbestic points is observed. The general kinetic technique is that previously described,[22,42,43] pseudofirst order conditions were used for the studies with $[Fe^{II}(CN)_6]^{4-}$ (reactions with the $\{Rh^{III}L_{15}\}^{3+}$ building block) or $S_2O_8^{2-}$ (reactions with Rh^{III}/Fe^{II} mixed valence compound) in excess.[44] The concentration of the mononuclear rhodium complex was kept in the $(3-8) \times 10^{-4}$ M range, while that of the Rh^{III}/Fe^{II} mixed valence complex was $(1-5) \times 10^{-4}$ M. Rate constants were found independent of its concentration and were determined by the use of Specfit global analysis software.[45] PIPPS[46] and borax buffer solutions were prepared at $I = 0.2$ M; final $I = 1.0$ M was achieved with $NaClO_4$ solution.[47] For pH = 0 experiments, a 1.0 M $HClO_4$ stock solution was used directly.

Atmospheric pressure runs were recorded on a Cary50 or a HP8453 instrument, equipped with a thermostatted multicell transport. For runs carried out at elevated pressures an already described pressurizing cell system setup was used connected to a TIDAS J&M instrument.[48,49] All the values obtained for the first order rate constants as a function of the metal complex, temperature, pressure, and different reactant concentrations are collected in the Supporting Information, Table S2.

Results and Discussion

Mononuclear Rh^{III} "Building Block" Complexes. The preparation of the mononuclear precursor complex, $\{Rh^{III}L_{15}\}$ indicated in Chart 2, was carried out as described in the literature.[30] The reaction produces, after ion exchange chromatography, a single compound comprising a pentadentate macrocycle in a *cis-VI* isomeric form according to the established nomenclature for cyclam-related macrocycles (Supporting Information, Chart S1).[36,50] Given the rich isomerization reactivity observed for Co^{III} and Cr^{III} complexes of the same family of ligands, the stability of this $\{Rh^{III}L_{15}\}$ unit in solution has been studied. As for the equivalent diamagnetic $\{Co^{III}L_n\}$ units, the ^{1}H NMR signal corresponding to the methyl group of the macrocycle (Chart 2) has proven an excellent spectroscopic signal for this purpose. In acidic medium the methyl resonance of *cis-VI*-$[RhClL_{15}]^{2+}$ at 1.35 ppm is unchanged, even when the temperature has risen to 60−70 °C for 24 h. When the complex is dissolved in 0.1 M NaOH the *cis-VI*-$[Rh(OH)L_{15}]^{2+}$ ion (obtained from chlorido hydrolysis),[30,51] undergoes a series of very slow isomerization reactions easily observed both by ^{1}H NMR and UV−vis spectroscopy (Figure 1). A ^{13}C NMR spectrum of the equilibrated solution is extremely complex and indicates the presence of some of the original *cis-VI* isomer of $\{Rh^{III}L_{15}\}$ plus the formation of two new species, the major having an asymmetric configuration (twelve ^{13}C NMR signals, possibly the *trans-II* isomer, with three amine protons on the same side of the macrocycle)

(38) Kern, S.; Illner, P.; Begel, S.; van Eldik, R. *Eur. J. Inorg. Chem.* **2010**, *2010*, 4658–4666.
(39) Farrugia, L. J. *J. Appl. Crystallogr.* **1999**, *32*, 837–838.
(40) Farrugia, L. J. *J. Appl. Crystallogr.* **1997**, *30*, 565.
(41) Wilkins, R. G. *Kinetics and Mechanisms of Reactions of Transition Metal Complexes*; VCH: Weinheim, 1991.
(42) Martínez, M.; Pitarque, M. A.; van Eldik, R. *J. Chem. Soc., Dalton Trans.* **1994**, 3159–3163.
(43) Martínez, M.; Pitarque, M. A. *J. Chem. Soc., Dalton Trans.* **1995**, 4107–4111.
(44) Espenson, J. H. *Chemical Kinetics and Reaction Mechanisms*; McGraw-Hill: New York, 1981.
(45) Binstead, R. A.; Zuberbuhler, A. D.; Jung, B. *SPECFIT32*, [3.0.34]; Spectrum Software Associates: Marlborough, MA, 2005.
(46) Jermyn, M. A. *Aust. J. Chem.* **1967**, *20*, 183–184.
(47) Perrin, D. D. *Aust. J. Chem.* **1963**, *16*, 572–578.
(48) Esteban, J.; Hirva, P.; Lahuerta, P.; Martínez, M. *Inorg. Chem.* **2006**, *45*, 8776–8784.
(49) van Eldik, R. *Inorganic High Pressure Chemistry*; Elsevier: New York, 1986; Chapter 1, pp 1−68.
(50) Bosnich, B.; Poon, C. K.; Tobe, M. L. *Inorg. Chem.* **1965**, *4*, 1102–1108.
(51) Hambley, T. W.; Lawrance, G. A.; Martínez, M.; Skelton, B. W.; White, A. L. *J. Chem. Soc., Dalton Trans.* **1992**, 1643–1648.

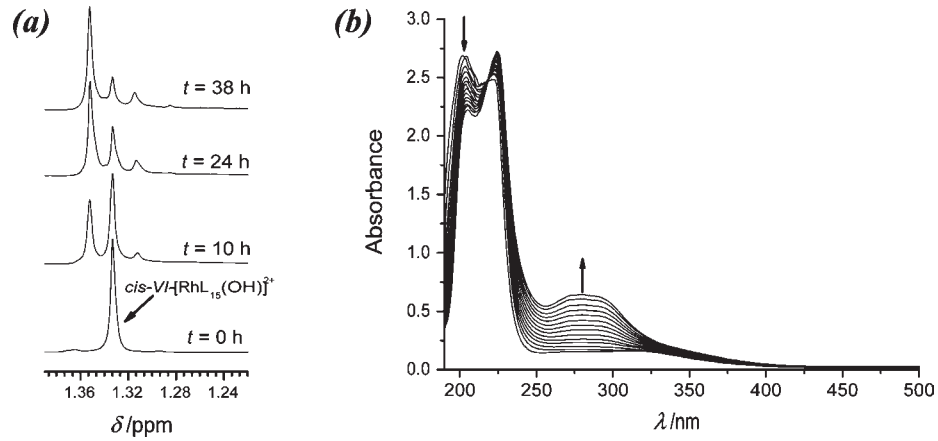

Figure 1. ^{1}H NMR (*a*) and UV−vis (*b*) spectroscopic changes observed for solution containing an hydrolyzed sample of *cis-VI*-$[RhClL_{15}]^{2+}$ at $T = 80$ °C.

and the minor having a mirror-plane symmetric arrangement (seven ^{13}C NMR signals, most likely the *trans-III* isomer; two protons above and two protons below the plane). ^{1}H NMR spectroscopy shows the two new isomeric forms maintaining a constant concentration ratio during the reaction, which is indicative of a relatively fast equilibrium established between these two. The final concentration ratio of the three species is set to 2/6/1 (*cis-VI*/asymmetric/symmetric). The *trans-II* and *trans-III* isomers are related by a single NH inversion, which should be facile in basic solution (Chart S1).

The UV−vis time monitored changes shown in Figure 1b at pH 11 and 12 indicate no $[OH^-]$-dependence of the observed first order rate constant (k_{obs}) as already established for the Co^{III} analogue compounds in this $[OH^-]$-saturated region according to eq 1.[36]

$$k_{obs} = K_{OS} \times k_{iso} \times [OH^-]/(1 + K_{OS} \times [OH^-]) \quad (1)$$

The values of these constants at different temperatures ($k_{iso} = 3.5 \times 10^{-6}$, 1.1×10^{-5}, and 3.2×10^{-5} s^{-1} at 60, 70, and 80 °C respectively) produced values of $\Delta H^{\ddagger} = 110 \pm 1$ kJ/mol and $\Delta S^{\ddagger} = -36 \pm 3$ J K/mol according to Eyring plots. These indicate a much less dissociative activation character than those determined for other base-hydrolysis reactions on Rh^{III}-amine complexes,[52,53] as well as for the analogous isomerization of the $\{Co^{III}L_{15}\}$ systems. The suitable fit of the Rh^{III} ion within the *cis-VI*-L_{15} cavity is probably responsible for this decrease in the dissociative activation nature of the process. Given the fact that this isomerization reactivity occurs over a much larger time scale than that observed leading to the mixed valent Rh^{III}/Fe^{II} species (see sections below) no further studies were carried out.

Reaction of $[Fe^{II}(CN)_6]^{4-}$ with *cis-VI*-$[Rh^{III}ClL_{15}]^{2+}$; a Redox Process. The reaction of $[Fe^{II}(CN)_6]^{4-}$ with the rhodium(III) mononuclear building block indicated above at pH 4 (thus avoiding any isomerization reactions of the $\{Rh^{III}L_{15}\}$ moiety itself) does not produce the expected mixed valence compound, $[\{cis\text{-}VI\text{-}L_{15}Rh^{III}(\mu\text{-}NC)\}Fe^{II}(CN)_5]^-$. Under these conditions the formation of a precipitate is observed with the simultaneous appearance of $[Fe^{III}(CN)_6]^{3-}$, indicated by the appearance of an intense band at 420 nm in the UV−vis spectrum. It is thus clear that the operation of the redox driven mechanism leading to the assembly of a dinuclear complex, generally observed for the Co^{III} analogues, does not lead to the desired dinuclear complex, yet a Rh^{III}/Fe^{II} redox reaction is still evident.[12,17,22] In the presence of EDTA no precipitate is observed. This suggests that, in the absence of EDTA, free Rh^{II} is formed (dissociated from L_{15}) which is precipitated by ferricyanide concomitant with reoxidation to Rh^{III} by air.[21,54,55] Given the inertness of the Rh^{III} complex precursor, reduction to the unstable divalent complex is the only conceivable explanation for dissociation of the complex, and this demands that ferrocyanide is the reductant in the absence of any other possibility.

The outer-sphere oxidation kinetics of $[Fe^{II}(CN)_6]^{4-}$ by *cis-VI*-$[Rh^{III}ClL_{15}]^{2+}$ was subsequently studied at pH 4 in the presence of 2−5 fold excess of EDTA to compare the data with that available for its Co^{III} and Cr^{III} analogues. The redox potential of *cis-VI*-$[Rh^{III}ClL_{15}]^{2+}$ could not be determined in water within the potential window set by the solvent, but the known value for $[Rh^{III}Cl(NH_3)_5]^{2+}$ of −750 mV[31] and the cathodic shift observed going from $[Co^{III}Cl(NH_3)_5]^{2+}$ to $[Co^{III}ClL_{14}]^{2+}$ (ca. −300 mV)[37] indicates a $Rh^{III/II}$ potential below about −1000 mV.[56] Thus, the fact that a redox reaction is even occurring is surprising given the $[Fe(CN)_6]^{3-/4-}$ potential (+465 mV).[15] It is well-known that the favorable electrostatic contribution resulting from the large opposing charges of the reactants (3+/4−) compensates for the unfavorable potentials.[12] The changes in the UV−vis spectrum (featuring the appearance of a maximum at 420 nm due to $[Fe^{III}(CN)_6]^{3-}$) at different $[Fe^{II}(CN)_6]^{4-}$ concentrations produced well-behaved kinetics. As seen in Figure 2a, k_{obs} saturates at high $[Fe^{II}(CN)_6]^{4-}$ values, as expected from a typical outer-sphere redox pseudo first order rate law (eq 2).[15,41,57]

$$k_{obs} = K_{OS} \times k_{et} \times [[Fe^{II}(CN)_6]^{4-}]/(1 + K_{OS} \times [[Fe^{II}(CN)_6]^{4-}]) \quad (2)$$

(52) Poe, A. J.; Vuik, C. *J. Chem. Soc., Dalton Trans.* **1976**, 661–666.
(53) Saliby, M. J.; Kaplan, E. B.; Sheridan, P. S.; Madan, S. K. *Inorg. Chem.* **1981**, *20*, 728–733.
(54) Gaswick, D.; Haim, A. *J. Am. Chem. Soc.* **1971**, *93*, 7347–7348.
(55) Rosenhein, L.; Speiser, D.; Haim, A. *Inorg. Chem.* **1974**, *13*, 1571–1575.
(56) Atkins, P.; Overton, T.; Rourke, J.; Weller, M.; Armstrong, F. A. *Inorganic Chemistry*; Oxford University Press: Oxford, England, 2006.
(57) Tobe, M. L.; Burgess, J. *Inorganic Reaction Mechanisms*; Longman: Harlow, England, 1999.

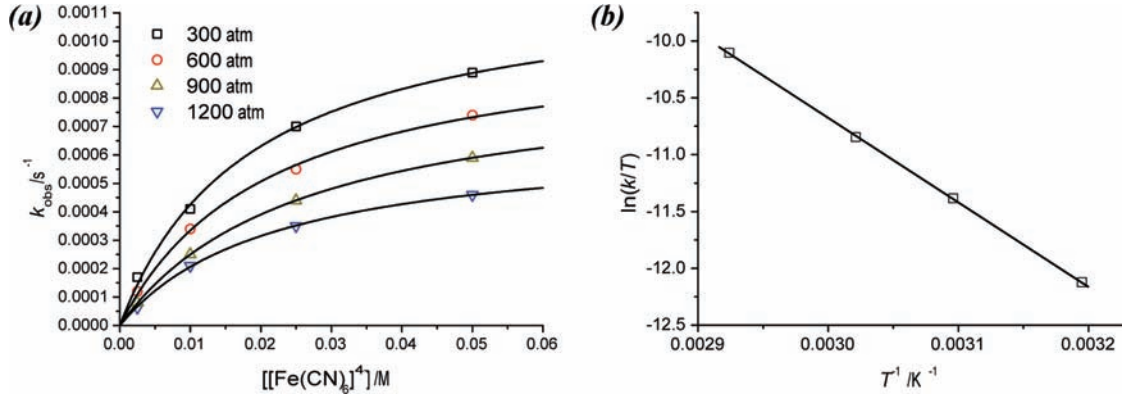

Figure 2. (*a*) Plots of the values of the pseudo first order rate constants, k_{obs}, obtained on reduction of *cis-VI*-$[Rh^{III}ClL_{15}]^{2+}$ with $[Fe^{II}(CN)_6]^{4-}$ at different pressures and at 40 °C (I = 1.0 M $NaClO_4$). (*b*) Eyring plot of $\ln(k_{et}/T)$ for the same process. Lines represent the best fit to the relevant equations.

Table 1. Kinetic and Activation Parameters for the Reactions of the Different $\{Rh^{III}L_{15}\}$ Building Blocks with $[Fe^{II}(CN)_6]^{4-}$ [a]

process	$\{Rh^{III}L_{15}\}$	$10^3 \times {}^{323}k$ /s^{-1}	K_{OS} [b] /M^{-1}	$\Delta H^{\ddagger}$ /kJ mol^{-1}	$\Delta S^{\ddagger}$ /J K^{-1} mol^{-1}	$\Delta V^{\ddagger}$ (T) /cm^3 mol^{-1} (K)	reference
O.S. redox	*cis-VI*-$[Rh^{III}ClL_{15}]^{2+}$	3.7	40	65 ± 1	−107 ± 4	39 ± 4 (313)	this work
O.S. redox	*trans-II/III*-$[Cr^{III}ClL_{15}]^{2+}$	5	10	120 ± 6	64 ± 20	25 ± 1 (308)	21
O.S. redox	*cis-VI*-$[Co^{III}(OH)L_{15}]^{2+}$	1.8 [c]	55	76 ± 3	−43 ± 10	20 ± 2 (298)	22
substitution	*cis-VI*-$[Rh^{III}(OH)L_{15}]^{2+}$	1.3 [d]		132 ± 3	89 ± 9	27 ± 1 (343)	this work
substitution	*trans*-$[Cr^{III}(OH)_2L_{15}]^{+}$	0.03	175	89 ± 4	−75 ± 11	−9.0 ± 0.3 (346)	21
substitution	*trans*-$[Cr^{III}(OH)_2L_{15}]^{+}$ [e]	0.21	170	96 ± 1	−36 ± 2	Not determined	21
substitution	*trans-I*-$[Co^{III}(OH)L_{14S}]^{+}$ [f]	0.18 [f]		131 ± 8	120 ± 17	Not determined	12
substitution	*trans-I*-$[Co^{III}(OH)L_{14S}]^{+}$ [g]	0.16 [g]		124 ± 6	97 ± 5	Not determined	12

[a] Relevant literature data for similar systems are also included. [b] Average for the temperatures studied. [c] At 298 K. [d] Second order rate constant $K_{OS} \times k$ /M^{-1} s^{-1}. [e] $[\{cis\text{-}V\text{-}L_{13}Co^{III}(\mu\text{-NC})\}Fe^{II}(CN)_5]^{-}$ as entering cyanido ligand. [f] $[\{trans\text{-}I\text{-}L_{14}Co^{III}(\mu\text{-NC})\}Fe^{II}(CN)_5]^{-}$ as entering cyanido ligand, second order rate constant (M^{-1} s^{-1}) determined under stoichiometric conditions. [g] $[\{trans\text{-}I\text{-}L_{14S}Co^{III}(\mu\text{-NC})\}Fe^{II}(CN)_5]^{-}$ as entering cyanido ligand, second order rate constant (M^{-1} s^{-1}) determined under stoichiometric conditions.

The variation of k_{et} with temperature and pressure produced the set of activation parameters collected in Table 1 (Figure 2b). The average value found for K_{OS} is of the same magnitude as that obtained for the equivalent Co^{III} and Cr^{III} systems analogue reactions.[21,22] As for the values found for the thermal activation parameters, these are similar to those obtained for the redox process involving Co^{III} centers, especially $\Delta H^{\ddagger}$, which does not agree with that expected from the redox potentials involved and the outer-sphere nature of the redox reaction. The $\Delta S^{\ddagger}$ value accounts for this discrepancy; the large degree of ordering on going to the transition state observed ($\Delta S^{\ddagger}$ = −107 J K^{-1} mol^{-1}) compensates the very unfavorable redox potentials. Furthermore, the large positive value obtained for $\Delta V^{\ddagger}$ indicates that we are dealing with an expansive ordering, typical for the involvement of hydrogen bonding interactions with the solvent in the transition state.[36,58] It is clear that the expansive disorganization expected on charge reduction ($\{Rh^{III\rightarrow II}ClL_{15}\}^{2+\rightarrow+}$ and $\{Fe^{II\rightarrow III}(CN)_6\}^{4-\rightarrow3-}$) does not account for the values obtained, as already observed for similar situations.[22,24,25,59,60]

Reaction of $[Fe^{II}(CN)_6]^{4-}$ with *cis-VI*-$[Rh^{III}(OH)L_{15}]^{2+}$; a Substitution Process. When the reaction described in the previous section was repeated at pH 11 neither precipitation nor any reaction occurs at short reaction times. When long reaction times or high temperatures are used some relevant changes take place at a time scales shorter (1 order of magnitude) than those needed for the isomerization process occurring on the starting *cis-VI*-$[Rh^{III}(OH)L_{15}]^{2+}$ (see before). The final UV−vis spectra for these reaction mixtures agree with that obtained for the complex $[\{cis\text{-}VI\text{-}L_{15}Rh^{III}(\mu\text{-NC})\}Fe^{II}(CN)_5]^{-}$ independently prepared (see below). The process produces kinetic absorbance versus time traces which obey a pseudo first order behavior. Figure 3a illustrates the trend observed for k_{obs} as a function of ferrocyanide concentration. From the linearity of the plot it is clear that the encounter complex formation equilibrium constant (K_{OS}) for the general rate law expected (eq 3) must have a rather small value (< 1 M^{-1})[41,57,61,62] (cf. Figure 2a) and indeed only the second order rate constant, $K_{OH} \times k_{subs}$, can be derived as the denominator of eq 3 is essentially unity($1 \gg K_{OS} \times [[Fe^{II}(CN)_6]^{4-}]$).

$$k_{obs} = K_{OS} \times k_{subs} \times [[Fe^{II}(CN)_6]^{4-}]/(1 + K_{OS} \times [[Fe^{II}(CN)_6]^{4-}]) \quad (3)$$

The variation of these constants with temperature and pressure produced the set of activation parameters collected in Table 1 (Figure 3b). The low value of K_{OS} is rather surprising, given the fact that the nature of the necessary outer-sphere encounter complex[41,57] is expected to be the same, independent of the process occurring inside the

(58) Bernhardt, P. V.; Gallego, C.; Martínez, M.; Parella, T. *Inorg. Chem.* **2002**, *41*, 1747–1754.
(59) Macpherson, B. P.; Alzoubi, B. M.; Bernhardt, P. V.; Martínez, M.; Tregloan, P.; van Eldik, R. *Dalton Trans.* **2005**, 1459–1467.
(60) Martínez, M.; Pitarque, M. A.; van Eldik, R. *J. Chem. Soc., Dalton Trans.* **1996**, 2665–2671.
(61) Martínez, M.; Ferrer, M. *Inorg. Chim. Acta* **1983**, *69*, 123–126.
(62) Martínez, M.; Ferrer, M. *Transition Met. Chem.* **1984**, *9*, 395–397.

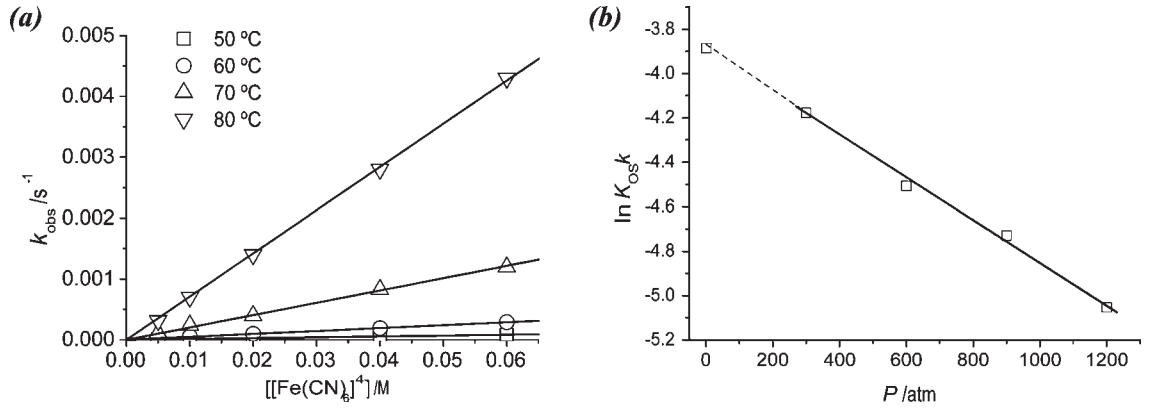

Figure 3. (*a*) Plots of the values of the pseudo first order rate constants, k_{obs}, obtained for the substitution of the OH^- group in *cis-VI*-$[Rh^{III}(OH)L_{15}]^{2+}$ by $[Fe^{II}(CN)_6]^{4-}$ at different temperatures (I = 1.0 M $NaClO_4$). (*b*) Plot of $\ln(K_{OS} \times k_{subs})$ versus P for the same process at 70 °C. Lines represent the best fit to the relevant equations.

solvent cage (i.e., the outer-sphere redox process indicated above).[63] Given the definite solvent assisted hydrogen bonding interactions existing in these systems, the fact that we are moving from a chlorido (hydrogen bonding acceptor) to an hydroxido ligand (hydrogen bonding both donor and acceptor) has to be necessarily related with this observation. The values found for the thermal and pressure activation parameters are not within the range of those found for the substitution reaction on other $\{Rh^{III}(N)_5\}$ cores.[64] The value of $\Delta H^{\ddagger}$ is considerably larger, while the values of $\Delta S^{\ddagger}$ and $\Delta V^{\ddagger}$ are indicative of an important degree of expansive disorganization on going to the transition state. This is surprising given the associative interchange character expected for the substitution processes on $\{Rh^{III}(N)_5\}$ cores.[65] It is possible that the sterically encumbered Rh^{III} center is responsible for this dissociative tuning of the activation.[29] Nevertheless, the fact that values of $\Delta S^{\ddagger}$ and $\Delta V^{\ddagger}$ necessarily contain unknown K_{OS} contributions, with a significant involvement of the solvent, makes these parameters less meaningful.

From the data in both Figures 2 and 3, the formation of mixed valence Rh^{III}/Fe^{II} complexes is mechanistically distinct from that observed for the Co^{III}/Fe^{II} analogues,[12,17,35] while similar to the process occurring for the formation of the Cr^{III}/Fe^{II} species.[21] The involvement of the solvent in outer-sphere hydrogen bonding interactions is a determining factor, both for the redox process to take place and for the activation parameters measured for the substitution process leading to the prototypical mixed valence $[\{cis\text{-}VI\text{-}L_{15}Rh^{III}(\mu\text{-NC})\}Fe^{II}(CN)_5]^-$ species.

Characterization of the Mixed Valence Rh^{III}/Fe^{II} Complex. Once the kinetic and mechanistic information of the reaction of the $\{Rh^{III}L_{15}\}$ building blocks with $[Fe^{II}(CN)_6]^{4-}$ was available, characterization of the final compound formed during the substitution reaction by $[Fe^{II}(CN)_6]^{4-}$ on *cis-VI*-$[Rh^{III}(OH)(L_{15})]^{2+}$ was pursued. The substitution process of the hydroxido ligand in *cis-VI*-$[Rh^{III}(OH)L_{15}]^{2+}$, obtained after base hydrolysis at pH 11,[30] by $[Fe^{II}(CN)_6]^{4-}$ was used for the preparation of the desired mixed valence $[\{cis\text{-}VI\text{-}L_{15}Rh^{III}(\mu\text{-NC})\}Fe^{II}(CN)_5]^-$ species, in a similar manner to that conducted for the preparation of $[\{trans\text{-}I\text{-}L_{14}Co^{III}(\mu\text{-NC})\}Fe^{II}(CN)_3(bpy)]^+$ or $[\{(OH)(HL_{15})Cr^{III}(\mu\text{-NC})\}Fe^{II}(CN)_5]^-$ species.[18,21] For these, the high redox potential of the iron $[Fe^{II}(CN)_4(bpy)]^{2-}$ center, or the susbtitutional lability of the Cr^{II} ion formed, prevented standard redox procedures used for other Co^{III} systems.[12,17] In the present case the instability of the intermediate Rh^{II} complex formed during the reduction of *cis-VI*-$[RhClL_{15}]^{2+}$ by hexacyanoferrate(II) contrasts with the redox inertness of *cis-VI*-$[Rh^{III}(OH)L_{15}]^{2+}$ with $[Fe^{II}(CN)_6]^{4-}$ and mirrors the chemistry observed for the for the analogous chromium system.

The anion exchange chromatographic procedures conducted on the reaction mixture reveal the expected small amounts of a positively charged trinuclear complex, probably $[\{cis\text{-}VI\text{-}L_{15}Rh^{III}(\mu\text{-NC})\}_2Fe^{II}(CN)_4]^{2+}$ by analogy with similar systems,[35] but this was not present in sufficient quantity for further characterization. Following a second chromatographic purification of the initial crude solid (see Experimental Section), the desired sodium salt of the $[\{cis\text{-}VI\text{-}L_{15}Rh^{III}(\mu\text{-NC})\}Fe^{II}(CN)_5]^-$ complex was obtained. Its ^1H NMR spectrum shows a single peak in the methyl region indicating its isomeric purity. ^{13}C NMR spectroscopy (Figure 4a) indicated the presence of the macrocyclic ligand in the expected *cis-VI* conformation (no isomerization) and three cyanide carbon signals at 184.1, 178.6, and 176.8 ppm are indicative of bridging, *cis*-to-bridge and *trans*-to-bridge cyanido ligands. The ^{13}C chemical shift values for the *cis*-to-bridge and *trans*-to-bridge ligands compare very well with those obtained for the equivalent Co^{III} complex,[34] but that for the bridging ligand itself is indicative of a smaller inductive effect of the larger Rh^{III} center with its associated lower charge density.

The UV−vis spectrum shows a new metal-to-metal charge transfer (MMCT Fe^{II} to Rh^{III}) electronic transition at 352 nm (1400 M^{-1} cm^{-1}) that disappears on $S_2O_8^{2-}$ oxidation (see below) and shifts to higher energies on protonation to $[\{cis\text{-}VI\text{-}L_{15}Rh^{III}(\mu\text{-NC})\}Fe^{II}(CN)_3(CN\mathbf{H})_2]^+$ in 1.0 M $HClO_4$ (Supporting Information, Figure S1).[17,24] The MMCT nature of this band has also been checked by solvatochromism (Supporting Information, Figure S2) where a significant shift of the maximum

(63) Burgess, J. *Ions in Solution*; Albion/Horwood: Chichester, England, 1999.
(64) Martínez, M.; Ferrer, M. *Inorg. Chem.* **1985**, *24*, 792–794.
(65) González, G.; Moullet, B.; Martínez, M.; Merbach, A. E. *Inorg. Chem.* **1994**, *33*, 2330.

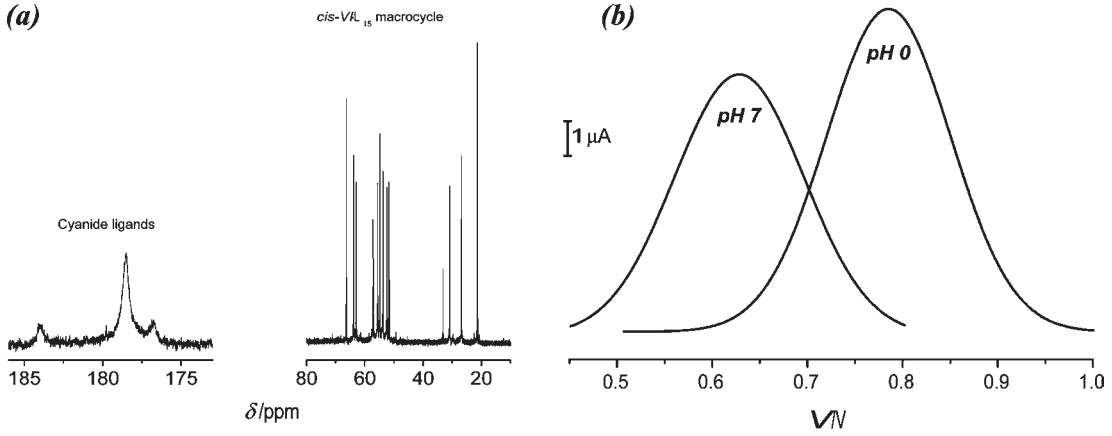

Figure 4. (*a*) ^{13}C NMR spectrum of species $[\{cis\text{-}VI\text{-}L_{15}Rh^{III}(\mu\text{-}NC)\}Fe^{II}(CN)_5]^-$ in D_2O at 25 °C and 100.6 MHz. (*b*) DPV signals of the $[\{cis\text{-}VI\text{-}L_{15}Rh^{III}(\mu\text{-}NC)\}Fe^{II}(CN)_5]^-$ (pH 7) and $[\{cis\text{-}VI\text{-}L_{15}Rh^{III}(\mu\text{-}NC)\}Fe^{II}(CN)_3(CNH)_2]^+$ (pH 0) (step 1 mV, 0.4 s; amplitude 50 mV, 0.04 s).

to longer wavelengths is observed on decreasing the polarity of the solvent.[15,66]

Cyclic voltammetry in water reveals the presence of a fully reversible $Fe^{III/II}$ redox couple at +630 mV (versus NHE) for the iron center, while no signal in the low potential range is observed, as expected for the redox inertness of the $Rh^{III/II}$ unit.[67] On acidification to 1.0 M $HClO_4$ the $Fe^{III/II}$ signal shifts to more positive values (785 mV) because of N-protonation of two cyanido ligands (Figure 4b).[24] The anodic shifts of these $Fe^{III/II}$ potentials relative[15] to the free $[Fe^{III/II}(CN)_6]^{3-/4-}$ are indicative of the attachment of a tripositive $\{Rh^{III}L_{15}\}$ block to the iron moiety (+420 → +630 mV) and subsequently because of two additional positive charges from protons introduced to two terminal cyanido ligands at pH = 0 (+630 → +785 mV). Nevertheless, the $Fe^{III/II}$ potentials are slightly more positively shifted than those obtained for the attachment of equivalent $\{Co^{III}L_n\}$ units. Given the larger size of the Rh^{III} center, and its consequent smaller inductive effect on the (μ-^{13}CN) NMR resonances, the differences may be related to a greater electronic coupling between the two centers, which increases the Fe^{III} character of the iron center of the mixed valence complex. In this respect the value determined for the extinction coefficient of the MMCT band at 352 nm (1400 M^{-1} cm^{-1}) is much larger than that of the Co^{III} analogue systems (ca. 500 M^{-1} cm^{-1}),[17] although not reaching that observed for the analogous Cr^{III}/Fe^{II} species (ca. 2800 M^{-1} cm^{-1}).[21] The orbital symmetry changes from a d^6/d^6 (t_{2g}^6:t_{2g}^6 → t_{2g}^5:$e_g^1t_{2g}^6$ Fe^{III}:Co^{II} excited state) to a d^6/d^3 system (t_{2g}^6:t_{2g}^3 → t_{2g}^5:t_{2g}^4 Fe^{III}:Cr^{II} excited state) have been held responsible for an increased value of the electronic coupling (H_{ab}) between the two centers in the latter case.[21] In the present example the intermediate extinction coefficient of the Rh^{III}/Fe^{II} complex cannot be rationalized as found for other $(Co^{III})_2/Fe^{II}$ and $(Co^{III})_3/Fe^{II}$ species.[12] The fact that Rh ion is a second row transition metal as opposed to its first row Co^{III} analogue metal may be relevant in influencing the larger MMCT extinction coefficient.

Reversible Redox Reactivity of the Mixed Valence Rh^{III}/Fe^{II} Complex. To fully compare this new system and its robustness with the already known $\{Co^{III}L_{15}\}$ analogues, the redox reactivity indicated in eqs 4−6 has been studied.

$$2[\{cis\text{-}VI\text{-}L_{15}Rh^{III}(\mu\text{-}NC)\}Fe^{II}(CN)_5]^- + S_2O_8^{2-} \rightarrow 2[\{cis\text{-}VI\text{-}L_{15}Rh^{III}(\mu\text{-}NC)\}Fe^{III}(CN)_5] + 2SO_4^{2-} \quad (4)$$

$$2[\{cis\text{-}VI\text{-}L_{15}Rh^{III}(\mu\text{-}NC)\}Fe^{II}(CN)_3(CNH)_2]^+ + S_2O_8^{2-} \rightarrow 2[\{cis\text{-}VI\text{-}L_{15}Rh^{III}(\mu\text{-}NC)\}Fe^{III}(CN)_5] + 2SO_4^{2-} + 2H^+ \quad (5)$$

$$2[\{cis\text{-}VI\text{-}L_{15}Rh^{III}(\mu\text{-}NC)\}Fe^{III}(CN)_5] + 2OH^- \rightarrow 2[\{cis\text{-}VI\text{-}L_{15}Rh^{III}(\mu\text{-}NC)\}Fe^{II}(CN)_5]^- + H_2O_2 \quad (6)$$

The reaction of the mixed valence $[\{cis\text{-}VI\text{-}L_{15}Rh^{III}(\mu\text{-}NC)\}Fe^{II}(CN)_5]^-$ species with peroxodisulfate, both at pH 4 and 0 (eq 4 and 5) produce significant changes in the UV−vis spectra (Figure 5a). The MMCT ($Fe^{II} \rightarrow Rh^{III}$) band vanishes, and the appearance of the $\{Fe^{III}(CN)_6\}$ chromophore is evident. The time course of these changes produced very well behaved kinetic traces that allowed for accurate determination of pseudo first order rate constants that varied linearly with the $[S_2O_8^{2-}]$ (Figure 5b) again because of a small and indeterminate K_{OS} value.

$$k_{obs} = K_{OS} \times k_{et} \times [S_2O_8^{2-}]/(1 + K_{OS} \times [S_2O_8^{2-}]) \quad (7)$$

Fitting these values to the rate law established for this type reaction according to eq 7 with $(1+K_{OS} \times [S_2O_8^{2-}]) \approx 1$, as for similar peroxodisulfate oxidations,[24,68,69] produced a set of temperature and pressure dependent second order ($K_{OS} \times k_{et}$) rate constants that gave the activation parameters indicated in Table 2. These are an

(66) Drago, R. S. *Physical Methods in Inorganic Chemistry*; Reinhold: New York, 1965.
(67) Curtis, N. J.; Lawrance, G. A.; Sargeson, A. M. *Aust. J. Chem.* **1983**, *36*, 1327–1339.
(68) Fagalde, F.; Katz, N. E.; Povse, V. G.; Olabe, J. A. *Polyhedron* **1998**, *18*, 25–31.
(69) Fürholz, U.; Haim, A. *Inorg. Chem.* **1987**, *26*, 3243–3248.

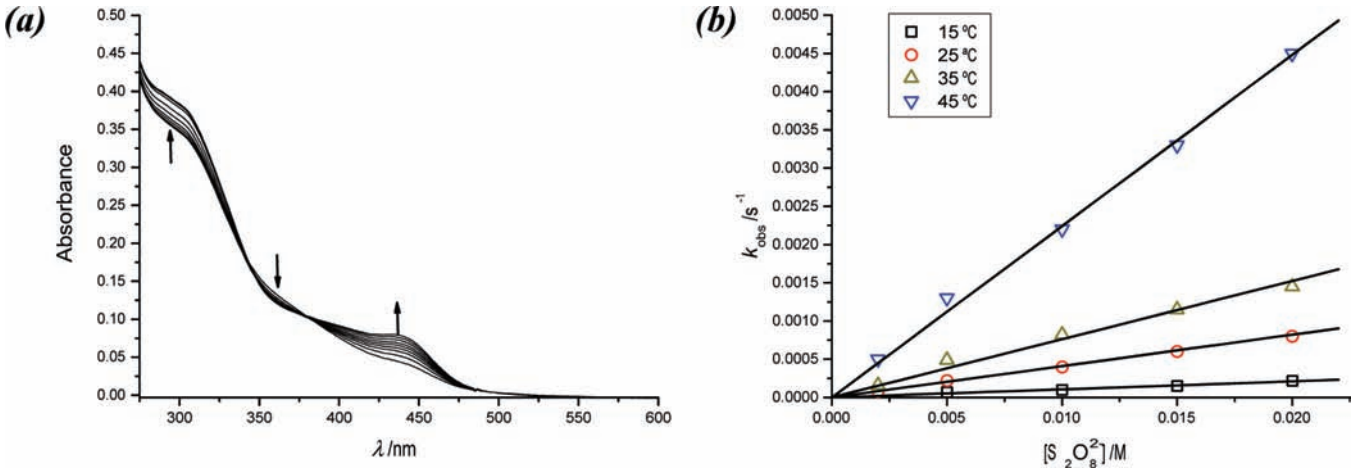

Figure 5. (*a*) UV−vis spectral changes observed on reaction of $[\{cis\text{-}VI\text{-}L_{15}Rh^{III}(\mu\text{-NC})\}Fe^{II}(CN)_5]^-$ with $S_2O_8^{2-}$ (25 °C, pH 4, I = 1.0 M $NaClO_4$). (*b*) Plot of the values obtained for k_{obs} for the oxidation of $[\{cis\text{-}VI\text{-}L_{15}Rh^{III}(\mu\text{-NC})\}Fe^{II}(CN)_5]^-$ with $S_2O_8^{2-}$ versus $[S_2O_8^{2-}]$ at different temperatures (pH = 4); the lines represent the best fit to the relevant equations.

Table 2. Kinetic and Activation Parameters for the Redox Reactions Involving the $[\{cis\text{-}VI\text{-}L_{15}Rh^{III}(\mu\text{-NC})\}Fe^{II}(CN)_5]^-$ Family of Complexes Complex in Different Media[a]

compound	reaction	^{298}k / M^{-1} s^{-1}	$\Delta H^{\ddagger}$ / kJ mol^{-1}	$\Delta S^{\ddagger}$ / J K mol^{-1}	$\Delta V^{\ddagger}$ (T) / cm^3 mol^{-1}(K)	reference
$[\{cis\text{-}VI\text{-}L_{15}Rh^{III}(\mu\text{-NC})\}Fe^{II}(CN)_5]^-$	$S_2O_8^{2-}$ oxdidation	0.035	78 ± 4	−26 ± 14	9 ± 1 (298)	this work
$[\{cis\text{-}VI\text{-}L_{15}Rh^{III}(\mu\text{-NC})\}Fe^{II}(CN)_3(CNH)_2]^+$	$S_2O_8^{2-}$ oxdidation	0.21	95 ± 8	54 ± 30	15 ± 1 (298)	this work
$[\{trans\text{-}III\text{-}L_{15}Co(\mu\text{-NC})\}Fe(CN)_5]^-$	$S_2O_8^{2-}$ oxdidation	0.16	55 ± 5	−76 ± 16	19 ± 2 (289)	24
$[\{trans\text{-}III\text{-}L_{15}Co(\mu\text{-NC})\}Fe(CN)_3(CNH)_2]^+$	$S_2O_8^{2-}$ oxdidation	0.17	90 ± 4	23 ± 15	11 ± 1 (289)	24
$[\{cis\text{-}VI\text{-}L_{15}Rh^{III}(\mu\text{-NC})\}Fe^{III}(CN)_5]$	OH^- reduction	3800 [b]	20 ± 1	−110 ± 5	30 ± 2 (293)	this work
$[\{trans\text{-}III\text{-}L_{15}Co^{III}(\mu\text{-NC})\}Fe^{III}(CN)_5]$	OH^- reduction	24000 [c]	15 ± 1	−113 ± 3	−9.6 ± 0.3 (288)	25
$[\{trans\text{-}I\text{-}L_{14}Co^{III}(\mu\text{-NC})\}Fe^{III}(CN)_5]$	OH^- reduction	200 [d]	28 ± 1	−108 ± 4	−8.9 ± 0.5 (288)	25

[a] Relevant literature data are also included. [b] Average K_{add} = 100 M^{-1}. [c] Average K_{add} = 26 M^{-1}. [d] Average K_{add} = 22 M^{-1}.

inseparable product of K_{OS} and k_{et}, and the values should be interpreted cautiously, specially taking into account the complicated nature of the outer-sphere complexes generated for these and other systems mentioned before.

The increased difficulty of oxidizing the Fe^{II} center upon protonation of two of the cyanido nitrogens (Figure 4b) accounts for the larger $\Delta H^{\ddagger}$ found for the oxidation of the $[\{cis\text{-}VI\text{-}L_{15}Rh(\mu\text{-NC})\}Fe(CN)_3(CNH)_2]^+$ complex, as already established for the analogous Co^{III} systems (Table 2). The value of $\Delta S^{\ddagger}$ also becomes more positive with the protonation of the mixed valence compound, the difference in the charge of the complexes involved in the formation of the outer-sphere precursor complex accounts for the difference. While at pH 4 the outer-sphere complex involves a {−1;−2} species, at pH 0 the formation of a {+1;−2} species and the consequent solvent liberation and entropy increase occurs. The values of $\Delta V^{\ddagger}$ show the same trend indicating that the changes of these parameters are due to solvation effects. The latter is in contrast with that observed for the Co^{III}/Fe^{II} analogues, indicated in Table 2. The larger coupling of the Rh^{III}/Fe^{II} pair reduces the negative charge on the $\{Fe(CN)_6\}$ subunit, thus decreasing electrostriction effects during the electron transfer to form the Rh^{III}/Fe^{III} pair that has been held responsible for the opposite trends of $\Delta S^{\ddagger}$ and $\Delta V^{\ddagger}$ for the Co^{III}/Fe^{II} analogues.[24]

Addition of NaOH to the above $S_2O_8^{2-}$ oxidized solutions immediately restored the mixed valence $[\{cis\text{-}VI\text{-}L_{15}Rh^{III}(\mu\text{-NC})\}Fe^{II}(CN)_5]^-$ complex, as has also been observed for the Co^{III} analogues (Supporting Information, Figure S3).[25] It is evident that the reversible redox reactivity observed for the $[\{LCo^{III}(\mu\text{-NC})\}Fe^{II}(CN)_5]^-$ complexes[25,28] is reproduced in the Rh^{III} analogue systems (eq 4 and 6). The reduction reaction rate for eq 6 is similar to that observed for the Co^{III}/Fe^{III} complexes, and the trends observed in the k_{obs} versus $[OH^-]$ plot are the same (Figure 6a), which is indicative of a reaction mechanism that has already been elucidated (Scheme 1).[17,25] The values of K_{add} (equilibrium constant for an $[\{cis\text{-}VI\text{-}L_{15}Rh^{III}(\mu\text{-NC})\}Fe^{III}(CN)_5];OH^-$ adduct formation) and those for $K_{dep} \times k_{et}$ (rate constant of the electron transfer process occurring on the deprotonated above-mentioned adduct) can be derived from the fitting of the data to eq 8.

$$k_{obs} = \frac{K_{add}K_{dep}k_{et}[OH^-]^2}{1 + K_{add}[OH^-] + K_{add}K_{dep}[OH^-]^2} \qquad (8)$$

These values, together with the pressure and temperature activation parameters obtained (Figure 6b) are also collected in Table 2.

The values of $\Delta H^{\ddagger}$ and $\Delta S^{\ddagger}$ are comparable with the data collected for the equivalent Co^{III}/Fe^{III} systems in reaction with hydroxide. It is clear that the slightly more favorable redox potential of the iron center in the Rh^{III}/Fe^{III} complex (see above) does not have a significant effect on the thermal activation parameters derived from the rate constants for the electron transfer process occurring on the $\{Rh^{III}/Fe^{III};OH^-\}$ adduct. The 4-fold difference in the values found for the equilibrium constant for

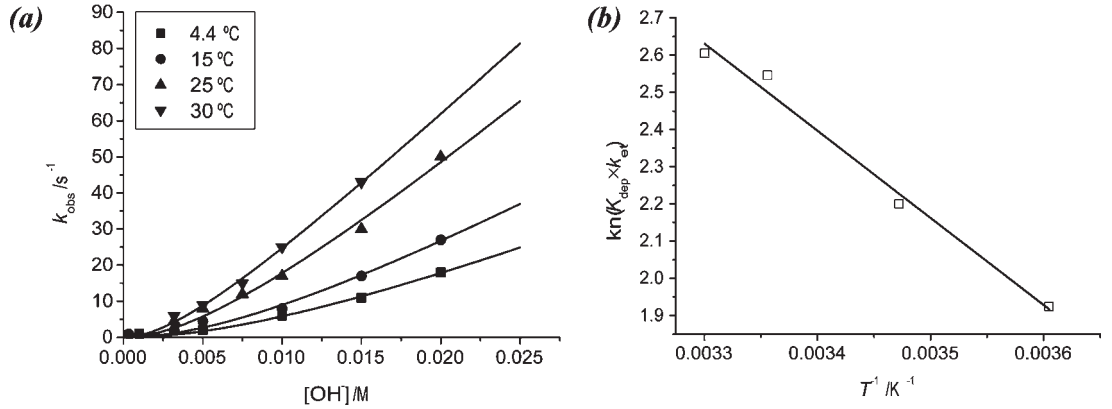

Figure 6. (*a*) Plot of the values obtained for k_{obs} versus [OH^-] for the reduction reactions of [{*cis-VI*-$L_{15}Rh^{III}$(μ-NC)}$Fe^{III}(CN)_5$] in alkaline medium at different temperatures. (*b*) Eyring plot for the temperature dependence of the $K_{dep} \times k_{et}$ constant for the reduction reaction of [{*cis-VI*-$L_{15}Rh^{III}$-(μ-NC)}$Fe^{III}(CN)_5$] in alkaline medium. I = 1.0 M $NaClO_4$.

Scheme 1

$$[LRh^{III}(NC)Fe^{III}(CN)_5]^0 + OH^- \underset{}{\overset{K_{add}}{\rightleftharpoons}} \{[LRh^{III}(NC)Fe^{III}(CN)_5]\cdot OH\}^- \quad (6.1)$$

$$\{[LRh^{III}(NC)Fe^{III}(CN)_5]\cdot OH\}^- + OH^- \overset{K_{dep}}{\rightleftharpoons} \{[LRh^{III}(NC)Fe^{III}(CN)_5]\cdot O\}^{2-} + H_2O \quad (6.2)$$

$$\{[LRh^{III}(NC)Fe^{III}(CN)_5]\cdot O\}^{2-} \xrightarrow{k_{et}} \{[LRh^{III}(NC)Fe^{II}(CN)_5]\cdot O^{\bullet}\}^{2-} \quad (6.3)$$

$$\{[LRh^{III}(NC)Fe^{II}(CN)_5]\cdot O^{\bullet}\}^{2-} \xrightarrow{fast} 1/2\ \{[LRh^{III}(NC)Fe^{II}(CN)_5]\cdot O\}_2^{4-} \quad (6.4)$$

$$1/2\ \{[LRh^{III}(NC)Fe^{II}(CN)_5]\cdot O\}_2^{4-} \xrightarrow{fast} [LRh^{III}(NC)Fe^{II}(CN)_5]^- + 1/2\ O_2^{\bullet 2-} \quad (6.5)$$

$$1/2\ O_2^{\bullet 2-} + H_2O \underset{}{\overset{K_a^{-1}}{\rightleftharpoons}} 1/2\ O_2H^- + OH^- \quad (6.6)$$

the preliminary adduct formation (K_{add}) should be viewed cautiously, given the large errors involved in their determination, and they cannot be related to inductive effects. Some other factors related with the outer-sphere H-bonding interactions are most likely responsible. As for the extremely positive value of $\Delta V^{\neq}$, it is in contrast with the values obtained for the Co^{III}/Fe^{II} analogues indicated in Table 2. Again, a very important difference in solvent interactions has to be involved in such dramatic differences, as already observed for the *cis-VI*-$[Rh^{III}(OH)L_{15}]^{2+}/[Fe^{II}(CN)_6]^{4-}$ substitution process mentioned before. As a whole the treatment of the mixed valence complex, [{*cis-VI*-$L_{15}Rh^{III}$-(μ-NC)}$Fe^{II}(CN)_5]^-$ in alkaline medium with $S_2O_8^{2-}$ produces H_2O_2 with no significant decomposition of the complex as has already been observed for the [{LCo^{III}(μ-NC)}$Fe^{II}(CN)_5]^-$ analogues.

Reaction of [{*cis-VI*-$L_{15}Rh^{III}$(μ-NC)}$Fe^{II}(CN)_5]^-$ with *trans-III*-$[CoClL_{14S}]^{2+}$: a Redox Process Assembling Heterotrinuclear [{*cis-VI*-$L_{15}Rh^{III}$(μ-NC)}{*trans-III*-$L_{14S}Co^{III}$-(μ-NC)}$Fe^{II}(CN)_4]^{2+}$. The robust character of the new [{*cis-VI*-$L_{15}Rh^{III}$(μ-NC)}$Fe^{II}(CN)_5]^-$ compound prompted us to pursue the formation of a novel heterotrinuclear $Rh^{III}/Fe^{II}/Co^{III}$ species using the original redox-assisted process we have employed for the preparation of [{*trans-II*-$L_{14}Co^{III}$(μ-NC)}{*trans-III*-$L_{14S}Co^{III}$(μ-NC)}$Fe^{II}(CN)_4]^{2+}$. Effectively the process follows the expected pathway comprising an outer-sphere redox process to produce the {[{*cis-VI*-$L_{15}Rh^{III}$(μ-NC)}$Fe^{III}(CN)_5$];*trans-III*-$[Co^{II}ClL_{14S}]^+$} successor complex which then undergoes a fast substitution to produce the thermodynamically unstable transient [{*cis-VI*-$L_{15}Rh^{III}$(μ-NC)}{*trans-III*-$L_{14S}Co^{II}$-

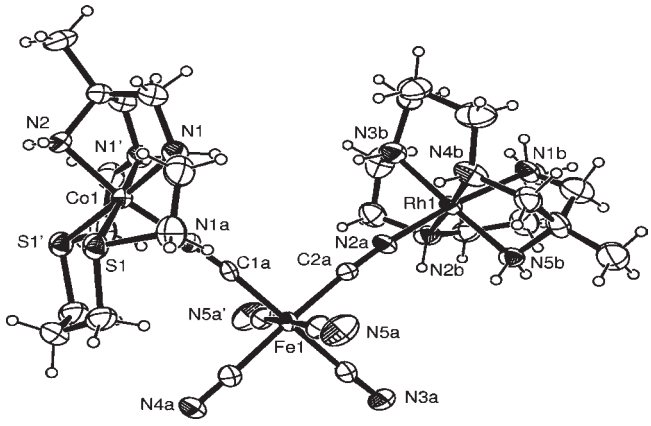

Figure 7. ORTEP view of the *cis*-[{*cis-VI*-$L_{15}Rh^{III}$(μ-NC)}{*trans*-III-$L_{14S}Co^{III}$(μ-NC)}$Fe^{II}(CN)_4]^{2+}$ cation (30% probability ellipsoids). Selected bond lengths (Å) Co1−N1a 1.902(8), Co1−N2 1.942(8), Co1−N1 1.971(6) Co1−S1 2.212(2), Fe1−C 1.88(1)−1.93(1), Rh−N2a 2.006(8), Rh1−N3b 2.031(17), Rh1−N5b 2.039(12), Rh1−N4b 2.042(16), Rh1 N1B 2.079(8), Rh1 N2B 2.082(15). Primes denote atoms related by mirror plane symmetry (x, $-y + 1/2$, z).

(μ-NC)}$Fe^{III}(CN)_4]^{2+}$ before rapid conversion to the final $Rh^{III}/Fe^{II}/Co^{III}$ complex.[12] The entire process is complete in 3 h at room temperature (despite the inherently inert low spin d^6 metal centers involved), in unbuffered pH and low ionic strength, as expected for a redox assisted reaction (via labile Co^{II}). Nevertheless, when the process is followed inside an electrochemical cell with I = 1.0 M $NaClO_4$ supporting electrolyte, the process only reaches about 50% completion after 24 h as expected from the important outer-sphere association constants found for these type of redox reactions.[21,23] The two products obtained after cation exchange chromatography agree with the expected presence of the two possible isomeric distribution of the two {$M^{III}L$} units (^{13}C NMR signals at 21.4; 26.8; 30.9; 51.7; 52.5; 53.7;54.8; 55.6; 57.2; 62.9; 63.8; 66.3 ppm for the {*cis-VI*-$L_{15}Rh$} moiety and at 21.8; 28.1; 34.5; 44.0; 58.4; 68.1; 71.6 ppm for the {*trans-III*-$L_{14S}Co$} units, respectively)[19,30,36] arranged around the central {$Fe(CN)_6$} unit, giving five ^{13}C NMR peaks at 173.4, 175.2, 180.2, 183.2, and 188.7 ppm for the *cis* form (including one accidental degeneracy) and three ^{13}C NMR signals at 174.7, 180.9, 191.5 ppm for the *trans*

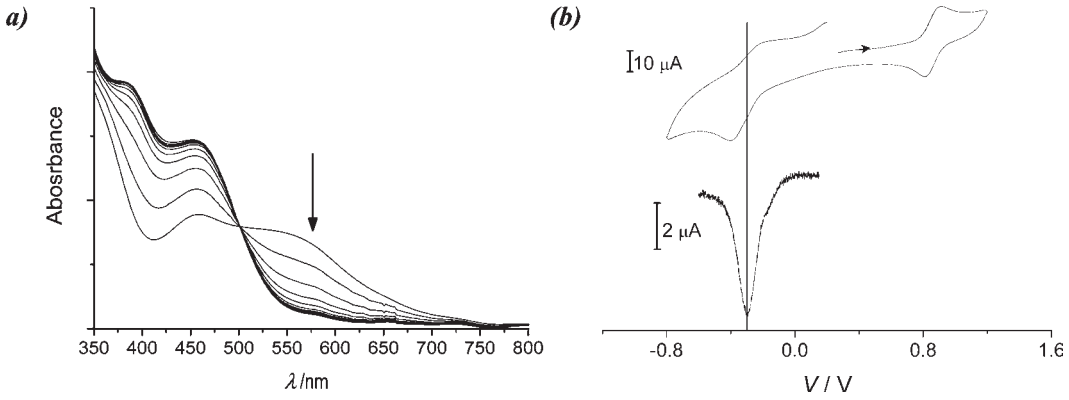

Figure 8. (*a*) Changes in the UV−vis spectrum in water of compound *trans*-[{*cis-VI*-$L_{15}Rh^{III}$(μ-NC)}{*trans-III*-$L_{14S}Co^{III}$(μ-NC)}$Fe^{II}(CN)_4]^{2+}$ upon $S_2O_8^{2-}$ oxidation. (*b*) Cyclic voltammogram (50 mV/s) and DPV (step 1 mV, 0.4 s; amplitude 50 mV, 0.04 s) of the same complex.

form) (Supporting Information, Figure S4). Furthermore, the non-statistical molar ratio of the *cis* and *trans* forms is consistent with the known preferential formation of *trans* isomers for complexes of this family such as *trans*-[{*trans-II*-$L_{14}Co^{III}$(μ-NC))}{*trans-III*-$L_{14S}Co^{III}$(μ-NC)}$Fe^{II}(CN)_4]^{2+}$ and *trans*-[{*trans-II*-$L_{14}Co^{III}$(μ-NC)}$_2$-$Fe^{II}(CN)_4]^{2+}$.[35]

The structure of the complex *cis*-[{*cis-VI*-$L_{15}Rh^{III}$-(μ-NC)}{*trans-III*-$L_{14S}Co^{III}$(μ-NC)}$Fe^{II}(CN)_4](ClO_4)_2\cdot 14H_2O$ was determined by X-ray crystallography. The molecular structure of the complex cation is illustrated in Figure 7. The cation and both perchlorate anions are situated on a crystallographic mirror plane, and one perchlorate is disordered between two orientations. It is apparent that the {*cis-VI*-$L_{15}Rh^{III}$(μ-NC)} moiety (where the primary amino group (N5b) is *cis* to the bridging cyanido ligand) is asymmetric and in fact this group is necessarily disordered about the mirror plane in its two enantiomeric forms (see Supporting Information, Figure S5) where only N2a and N1b lie on the mirror plane. The {$Fe^{II}(CN)_6$} and {*trans-III*-$L_{14S}Co^{III}$(μ-NC)} moieties, each with local C_s symmetry, are properly ordered about the mirror plane. A number of water molecules (a total of fourteen per cation) are also present in the asymmetric unit.

Each d^6 metal ion is six-coordinate. The $Rh-N_{amine}$ bond lengths are typical of hexaamine analogues[70] while the bridging Rh-NC bond is the shortest. In the folded (*cis*) conformation of the L_{15} macrocycle the secondary amine donors are found in the *R*(N1B)*R*(N2B)*S*(N3B)-*R*(N4B) (and enantiomeric *SSRS*) form which has been previously defined as *cis-VI*[12] in keeping with the traditional conventions of cyclam-related macrocyclic amines.[50] The Co center is found in the *trans-III* configuration with the bridging cyanido N-donor (N1a) *trans* to the pendant primary amine (N2). The secondary amine H-atoms are necessarily on the opposite side of the CoN_2S_2 plane to the primary amine (N2) while the S-atom lone pairs are *syn* with respect to the pendent amine. The Co−S and Co−N bond lengths are unaffected by introduction of the N-bound ferrocyanide unit, as noted previously.[19] The Rh−N bond lengths are not significantly different from those found in *cis-VI*-[RhClL_{15}]$(ClO_4)_2\cdot H_2O$.[30] The ferrocyanide moiety also exhibits bond lengths typical of its parent mononuclear and dinuclear analogues.[19,27,34,37,71] The $Fe^{II}-CN-Co^{III}$ distance is the longest from all the complexes of this family that have been crystallographically characterized. The relative positions of the two macrocyclic moieties are such that the possible steric constrains are minimized.

UV−vis spectroscopy and electrochemistry (Figure 8) indicate the mixed valence nature of this new species. In the UV−vis spectra the MMCT bands for both the Fe^{II}-to-Co^{III} (*trans* 540 nm (ε = 555 M^{-1} cm^{-1}) and *cis* 550 nm (ε = 550 M^{-1} cm^{-1})) and Fe^{II}-to-Rh^{III} (*trans* and *cis* 352 nm (ε = 1300 M^{-1} cm^{-1})) are evident. Both MMCT bands are very similar in position and intensity to those found for the respective dinuclear precursor compounds; $Fe^{II} \rightarrow Rh^{III}$, 352 nm ($\varepsilon$ = 1120 M^{-1} cm^{-1}) and $Fe^{II} \rightarrow Co^{III}$, 565 nm ($\varepsilon$ = 520 M^{-1} cm^{-1}).[19] The values found for the reversible redox responses from the iron and cobalt centers follow the trend established for this family of complexes (ca. 200 mV anodic shift for the $Fe^{III/II}$ pair on incorporation of a tricationic {$M^{III}L$} unit to the iron center and about 100 mV decrease for the $Co^{III/II}$ pair on incorporation of the anionic {$Fe^{II}(CN)_6$} unit of the mixed valence complex).[17] As before the electrochemical experiments do not show the redox response associated with the $Rh^{III/II}$ couple, as expected from literature data and our results on the simpler mono and dinuclear precursors.[67]

Conclusions

The formation of new dinuclear Rh^{III}/Fe^{II} and heterotrinuclear $Rh^{III}/Fe^{II}/Co^{III}$ mixed valence compounds has been achieved via a combination of the well established redox-assisted process operating for the related Co^{III}/Fe^{II} assemblies and a direct substitution process as used for the formation of Cr^{III}/Fe^{II} units. The new compounds formed show a set of MMCT bands that correspond to the convolution of the two separate M^{III}/Fe^{II} units, and their electrochemistry also agrees with the presence of the separate units. The redox chemistry on the {$Fe^{II}(CN)_6$} moiety of both the Rh^{III}/Fe^{II} and the $Rh^{III}/Fe^{II}/Co^{III}$ complexes parallels that observed for the $Co^{III}{}_3/Fe^{II}$ and $Co^{III}{}_2/Fe^{II}$ species. The complexes *trans*- and *cis*-[{*cis-VI*-$L_{15}Rh^{III}$(μ-NC)}{*trans-III*-$L_{14S}Co^{III}$(μ-NC)}-$Fe^{II}(CN)_4]^{2+}$ are unprecedented examples of heterotrinuclear

(70) Bernhardt, P. V.; Lawrance, G. A.; Hambley, T. W. *J. Chem. Soc., Dalton Trans.* **1990**, 983–987.

(71) Bernhardt, P. V.; Macpherson, B. P.; Martínez, M. *Inorg. Chem.* **2000**, *39*, 5203–5208.

mixed valent compounds based on ferrocyanide. The systematic assembly of these subunits via these established redox-assisted and direct substitution approaches demonstrates the utility of this methodology. It is now apparent that the designed assembly of mixed-metal complexes such as these demands a rational mechanistic approach. The presence of disparate electron acceptor units (Co^{III} and Rh^{III}) within the same mixed valent ferrocyanide complex represents a novel example of a compound exhibiting vastly different MMCT transitions and presents new challenges for theoreticians and spectroscopists in the area of mixed valence chemistry.

Acknowledgment. Financial support for this work was provided by DGI, Grant CTQ2009-14443-C02-02.

Supporting Information Available: Observed rate constants, k_{obs}, for the reactions studied, crystallographic data in CIF format, and figures of kinetic, spectroscopic, and crystallographic data. This material is available free of charge via the Internet at http://pubs.acs.org.